Instability of a crystal ^{4}He facet in the field of gravity

S. N. Burmistrov, L. B. Dubovskii, V. L. Tsymbalenko
Kurchatov Institute, 123182 Moscow, Russia

We analyze the analog of the Rayleigh instability in the field of gravity for the superfluid-crystal ^{4}He interface provided that the heavier ^{4}He crystal phase occupies the half-space over the lighter superfluid phase. The conditions and the onset of the gravitational instability are different in kind above and below the roughening transition temperature when the crystal ^{4}He surface is in the rough or in the smooth faceted state, respectively. In the rough state of the surface the gravitational instability is similar to the classical case of the fluid-fluid interface. In contrast, in the case of the crystal faceted surface the onset of the gravitational instability is associated with surmounting some potential barrier. The potential barrier results from nonzero magnitude of the linear facet step energy. The size and the tilting angle of the crystal facet are also important parameters for developing the instability. The initial stage of the instability can be described as a generation of crystallization waves at the superfluid-crystal interface. The experiments which may concern the gravitational instability of the superfluid-crystal ^{4}He interface are discussed.

PACS numbers: 67.80.bf, 47.20.Ma

I. INTRODUCTION

The Rayleigh instability is a well-known instability of the interface between two liquids in the field of gravity when the heavier liquid is placed above the lighter one. The similar effect is difficult to observe in solids since any displacement of a piece of the solid body is impeded due to appearing elastic stresses. However, there exists an elastic stress-free possibility of changing the shape of a crystal, namely, remelting in the hydrostatic pressure gradient. A ^{4}He crystal in contact with its superfluid phase could be one of most promising objects to observe the manifestation of the Rayleigh instability for the liquid-solid interface. In fact, solid ^{4}He density is larger than that of the liquid phase. The growth rate of atomically rough crystal surfaces increases drastically with the lowering of the temperature, and the change of the crystal shape can occur in very short time intervals of about 1 s. Unfortunately, in most of crystal growth experiments [1] a ^{4}He crystal appears either at the bottom of an experimental cell or drops on the same bottom later if a crystal seed nucleates first at the wall. Thus, preparing the necessary configuration with the heavier crystal above its lighter liquid phase in order to have the initial condition for the development of the classical Rayleigh instability comes across a difficulty.

Nevertheless, one experiment, in which the necessary liquid-crystal configuration against the direction of gravity is arranged, has been reported [2]. A single hcp ^{4}He crystal is grown at the bottom of an experimental cell at the temperature of about 1.1 K lying between the first and second roughening transitions. After the grown ^{4}He crystal occupies the lower half of the optical cell, the cell is rotated mechanically through 180° so that the ^{4}He crystal proves to be above the superfluid liquid. Then the crystal phase starts to melt, descending along the cell walls. In its turn, a single finger of the superfluid phase moves in the upward direction at the center of the cell. Eventually, the crystal again occupies the lower half of the cell. Unfortunately, the development of the instability observed is described qualitatively and the results of visual observations are illustrated by the schematic figure alone. The main conclusion of the work is that the spatial scale associated with the development of the instability is about 1 cm.

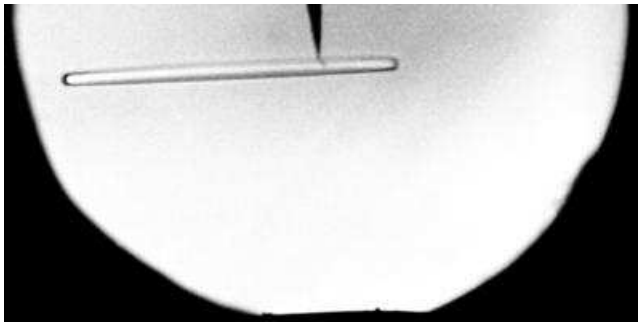

FIG. 1: The ^{4}He crystal grown at 0.92 K between two roughening transitions as in experiment [3]. The diameter of the visible margin is 12 mm.

This result [2] seems to conflict with the stability observed for the lower surface of the ^{4}He crystals grown on the needle point at the center of a cell (Fig. 1). As is seen from the figure, the lower crystal facet is under conditions appropriate for the development of the gravitational Rayleigh instability. The single distinction is likely to be associated with the state of the crystal ^{4}He surface. Whereas in experiments [2] one deals with the rough state of the crystal ^{4}He surface, in our experiments [3] one observes the smooth faceted state of the surface in the form of a hcp crystal basal facet above the superfluid phase.

In this paper we consider an instability of the crystal ^{4}He surface above the superfluid phase in the field of gravity. We analyze and compare two possible states of the crystal ^{4}He surface such as the rough and smooth faceted ones.

II. INSTABILITY OF THE CRYSTAL SURFACE IN THE ROUGH STATE

We start our consideration from the high temperature region above the roughening transition when the crystal surface is in the atomically rough state. Since in this case the surface tension α has no singularity at the close-packed facets and weakly depends on the crystallographic direction, the tensor of surface stiffness γ_{ik} is close to $\alpha\delta_{ik}$. Thus, to simplify the analysis, we neglect any distinction between surface tension and surface stiffness in the formulas for the Laplace pressure.

A. Flat shape of the crystal surface

Crystallization waves, representing small oscillations of the superfluid-solid ^{4}He interface, are predicted by Andreev and Parshin [4]. The spectrum of crystallization waves in the field of gravity can be found from the equation [5]

$$\rho_{\rm ef}\,\frac{\omega^2}{q}+i\frac{\rho'}{K}\,\omega-\alpha q^2-\Delta\rho g=0,\quad \rho_{\rm ef}=\frac{(\Delta\rho)^2}{\rho}\,. \qquad (1)$$

Here q is the wave vector, $\Delta\rho=\rho'-\rho$ where ρ' and ρ are the densities of the solid and liquid phases, K is the interface growth coefficient, and g is the acceleration of gravity. The positive magnitude $g>0$ corresponds to the usual situation when the ^{4}He crystal lies under the liquid phase. In this case the frequencies of small interface oscillations have the negative imaginary parts for all wave vectors and the crystal surface is always stable.

Provided the solid phase occupies the half-space above the liquid, the dispersion equation remains the same but parameter g becomes negative. This means that the last term in (1), which dominates for sufficiently small q, can result in the positive imaginary part for the roots of the dispersion equation. The critical magnitude of the wave vector q_0 is given by

$$q_0=\sqrt{\frac{\Delta\rho\,g}{\alpha}}=1/\lambda,$$

where $\lambda\sim$1 mm is the capillary length. The instability will develop faster for small wave vectors. For the harmonic $q\to 0$, the estimate for the time of developing the instability is given by

$$t\sim\frac{\rho'}{\Delta\rho}\,\frac{1}{gK}\,. \qquad (2)$$

For $T\sim$1.1 K, the inverse growth coefficient $1/K\sim 2$ m/s and $t\sim 2$ s. This is in a qualitative agreement with the observations of work [2]. Thus, the instability similar to the Rayleigh one develops at the lower surface of a ^{4}He crystal in the atomically rough state.

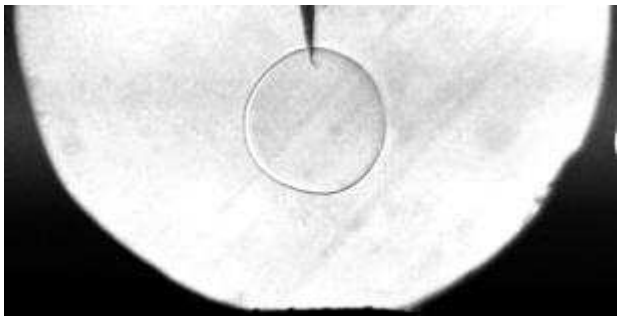

FIG. 2: The isotropic growth of a ^{4}He at 1.28 K. The diameter of the visible margin is 12 mm.

B. Spherical shape of a solid

An interesting situation appears with the nucleation and growth of a crystal at the needle point at the temperatures above the roughening transitions (Fig. 2). In the hydrostatic pressure gradient the crystal grows in the shape of a ball which melts in the upper part and crystallizes in its lower part at the same time. In outward appearance this looks like the motion of a crystal downward. In work [3], in which the similar situation is studied, it is shown that the crystal with the isotropic growth coefficient conserves its spherical shape, and the descending motion velocity of the sphere v is equal to

$$v=K\,\frac{\Delta\rho}{\rho}\,gR(t), \qquad (3)$$

where $R(t)$ is a time-dependent radius of the sphere. Then, as follows from (3), the center of the crystal shifts downward at a constant velocity in the hydrostatic pressure gradient provided the crystal volume remains unchanged.

Let us consider stability of the spherical shape of a crystal against small shape perturbations in the field of gravity. For analysis, we choose the frame which origin is put at the center of a crystal. In this frame the center of a crystal is fixed and the liquid phase circulates around the crystal, outflowing from the upper part of the sphere and flowing into the sphere in its lower part. We introduce $\zeta(t)\ll R$ as a small perturbation of the radius $R(t)$. The liquid phase is assumed to be incompressible and the solid one is motionless. In experiment [3] the velocities of the liquid flow are small and do not exceed 0.1 mm/s. For the hydrodynamic pressure $\rho v^2/2$, we have an estimate 10^{-2} dyne/cm^2. This magnitude is much smaller than the typical hydrostatic pressure drop $\Delta\rho\,gR$. In what follows, we neglect quadratic terms in velocity of the liquid phase.

Next, in accordance with the experimental conditions, we take into account that the experimental cell is closed and no matter comes from outside. In other words, the total mass of the liquid and solid phases remains unchanged. In the frame comoving with the crystal the center of the crystal is fixed. As a result, we can omit

the spherical harmonic with $l = 0$ from consideration since this harmonic is associated with the change of the volume. The next harmonic $l = 1$ is responsible for the displacement of the sphere as a whole and corresponds to the circulation of the liquid around of the sphere. We also omit this harmonic from our consideration.

The determination of the oscillation spectrum is not difficult but cumbersome. We give a scheme of solution and then the final result. Let axis z run in the vertical direction, and we seek for the general solution, expanding perturbation ζ in spherical harmonics. Since the liquid is assumed to be incompressible, it is convenient to describe its motion in terms of velocity potential ϕ according to $\boldsymbol{v} = \nabla\phi$. The mass flow across the interface is proportional to the chemical potential difference $\Delta\mu$

$$J = \rho' K \Delta\mu.$$

The continuity of the mass flow across the interface allows us to relate the velocity of the liquid at the interface with the interface growth rate $\dot{\zeta}$. After some calculations and involving the axial symmetry with respect to axis z, we arrive eventually at the dispersion relation

$$\left[\frac{\omega^2}{\omega_0^2} + i\omega\,\frac{\Gamma}{\omega_0^2}(l+1) - (l-1)(l+1)(l+2)\right]a_l - \frac{2R^2}{\lambda^2}\left[\frac{l^2}{4l^2-1}\,a_{l-1} + \frac{(l+1)(l+2)}{(2l+1)(2l+3)}\,a_{l+1}\right] = 0, \quad (4)$$

where

$$\omega_0^2 = \frac{\alpha}{R^3}\,\frac{\rho}{(\Delta\rho)^2}\,, \quad \Gamma = \frac{\rho\rho'}{(\Delta\rho)^2}\,\frac{1}{KR}\,, \quad (5)$$

and a_l is the perturbation amplitude corresponding to l-th spherical harmonic from a sum $\zeta(t) = \sum_l a_l(t)Y_l$. Thus, we have a determinant of the infinite order for determining the proper values. In the lack of gravity $\lambda = \infty$ the off-diagonal terms vanish. The roots of the master equation give the oscillation spectrum of a spherical solid with damping. All the frequencies have a negative imaginary part, resulting in the conclusion that in this case the spherically shaped solid is stable against small perturbations of its equilibrium shape.

In the presence of gravity we must involve the off-diagonal terms in (4). Note that the diagonal terms increase proportional to l^3 as $l \to \infty$, while the off-diagonal terms remain finite and have the order of $(R/\lambda)^2$. This means that, as the degree of harmonic l increases, the relative effect of the pressure gradient reduces, agreeing with the stability of the flat interface at large wave vectors. As in the case of the flat interface, the instability develops in the first turn for the minimum degree of harmonics $l = 2$.

The spherical shape of helium crystals in the hcp phase is observed above the first roughening transition temperature at $T >$1.25 K (Fig. 2). On the other hand, the hcp phase is limited by the hcp-bcc transition at $T =$1.44 K.

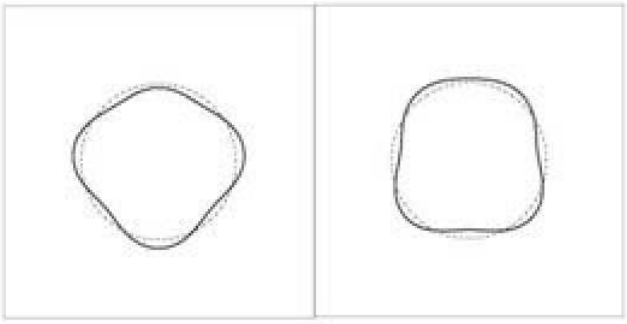

FIG. 3: The initial stage for the development of instability for a spherical crystal with the size larger than the critical radius. The dashed circle is the initial shape.

Within this temperature range the kinetic growth coefficient is small and varies insignificantly with the temperature from $1/K \sim$11 m/s at the bcc transition to $\sim$3 m/s near the roughening transition. Inserting these values into Eqs. (4, 5) and solving numerically the master equation for proper frequencies, we determine the critical radius $R_c =$0.61 cm. The radius of crystals studied in [3] does not exceed this magnitude. This may serve as an explanation that all the crystals grown in that experiment display stability of their spherical shape.

The proper vectors in (4) are determined with accuracy to their sign. For $R > R_c$, this gives two possible cases for developing the instability shown in Fig. 3. In the first case at the bottom there appears a hogging in the upward direction. In the second case we see a formation of constriction. Note that the result refers only to the initial stage of developing instability.

C. Crystals of the limited sizes

Another factor which stabilizes the flat surface is a finiteness of the crystal size. In this case the spectrum of crystallization waves becomes discrete. The instability will appear at the minimum wave vector. To estimate, we replace the hexagonal crystal shape with the equivalent cylindrical one of radius R. Then we can show that dispersion equation (1) holds its form but the perturbation amplitude ζ of the flat crystal surface is given by

$$\zeta(\boldsymbol{r},\, t) = \zeta_0 J_m(qr)\, e^{im\phi} e^{-i\omega t},$$

where ϕ is the azimuth angle, J_m is the Bessel function, and r is the distance from the center of a cylinder. For the circular symmetry at the fixed volume of a crystal, the minimum wave vector q_0 is determined from the relation

$$J_1(q_0 R) = 0, \quad q_0 \approx 3.83/R\,. \quad (6)$$

From expressions (1–2) and (6) one can obtain that the instability should appear for a crystal with the diameter larger than 6 mm.

III. INSTABILITY OF A CRYSTAL FACET

Below the roughening transition temperature a singularity appears as a nonanalytic angular dependence in the behavior of the surface tension versus angle θ between the direction of crystallographic axis and the normal to the crystal surface [6]

$$\alpha(\theta) = \alpha_0 + \beta(T) \mid \theta \mid + \cdots, \quad (|\theta| \ll 1).$$

Here β is the quantity proportional to the energy of a crystal facet step and is positive below the roughening transition temperature. This entails that the surface tension and surface stiffness represent the drastically different quantities. The surface stiffness becomes infinite for zero angle $\theta = 0$. The singularity prevents from varying the shape of the crystal facet and qualitatively changes the conditions for stability. Let us consider the distinctions in appearing the Rayleigh instability in comparison with the case of the rough crystal surface.

A. Rayleigh instability of the horizontal crystal facet

Below the roughening transition the energy variation of the surface for sufficiently small perturbation amplitude $\zeta(x, y)$ from the horizontal flat facet is equal to

$$\Delta E = \int \left(\frac{\alpha_0}{2} (\nabla\zeta)^2 + \beta \mid \nabla\zeta \mid - \frac{\Delta\rho\, g}{2} \zeta^2 \right) dx\, dy.$$

The smallness of ζ and $\nabla\zeta$ for the correct and consistent use of the expansion of energy in ζ is provided by inequality $\beta \ll \alpha_0$. Let us start from the one-dimensional case, namely, flat bar of length L. The energy per unit length $\Delta E/D$ reads

$$\frac{\Delta E}{D} = \int\limits_{-L/2}^{L/2} \left(\frac{\alpha_0}{2} \left(\frac{\partial\zeta}{\partial x} \right)^2 + \beta \left| \frac{\partial\zeta}{\partial x} \right| - \frac{\Delta\rho\, g}{2}\, \zeta^2 \right) dx,$$

where D is the width of the crystal bar in the transverse direction. The boundary conditions at the ends of the bar

$$\zeta(-L/2) = \zeta(L/2) = 0 \tag{7}$$

correspond to the case when the crystal surface is immobile at these points. It is convenient to introduce the dimensionless quantities according to $x' = x/L$, $\eta = \zeta(\Delta\rho\, gL)/\beta$, and $\gamma = \lambda/L$. Then,

$$\frac{\Delta E[\eta(x')]}{D} = \frac{\beta^2}{\Delta\rho\, gL} \int_{-1/2}^{1/2} \left(\frac{\gamma}{2} \eta'^{\,2} + \mid \eta' \mid - \frac{\eta^2}{2} \right) dx'$$

The extremum satisfies the equation

$$\gamma^2 \eta'' + 2\delta(\eta')\eta'' + \eta = 0.$$

Two types of functions can be solutions of the equation

$$\eta(x') = \eta_0 \left\{ \begin{array}{c} 1 \\ \sin(x' - x_0')/\gamma \end{array} \right. ,$$

i.e., either a constant or a sine function.

The height of a potential barrier for destructing the flat crystal facet as well as the type of a critical fluctuation depend on the magnitude γ. For sufficiently small length of the facet $L < L_{c1} = \pi\lambda$, there exists a single trivial solution $\eta(x') = 0$, and the flat crystal facet remains stable. For $L > L_{c1}$, there appears a nontrivial solution which consists of two half-sinusoids and flat segment

$$\eta(x') = \eta_0 \left\{ \begin{array}{ll} 1\,, & \mid x' \mid \leqslant x_0' = \frac{1-\pi\gamma}{2} \\ \sin\frac{1/2 - |x'|}{\gamma}\,, & x_0' < \mid x' \mid \leqslant 1/2 \end{array} \right. .$$

Here the function $\eta(x')$ is continuous together with its derivative at points $x' = \pm x_0'$ and vanishes at $x' = 1/2$. The critical perturbation amplitude of fluctuation is equal to

$$\eta_{c1} = \frac{2}{1 - \pi\gamma} \quad \text{or} \quad \zeta_{c1} = \frac{2\beta}{\Delta\rho\, g}\, \frac{1}{L - L_{c1}}\,.$$

The height of the potential barrier, separating the transition of the flat crystal facet to a distorted state, is given by

$$\frac{\Delta E}{D} = \frac{2}{1 - \pi\gamma} = \frac{2\beta^2}{\Delta\rho\, g}\, \frac{1}{L - L_{c1}}\,. \tag{8}$$

As the size of a crystal facet increases, there appear additional possibilities for other fluctuations consisting of a combination of flat segments and half-sinusoids. The corresponding solutions, composed with n flat segments, appear as $L > L_{c\,n}$ where $L_{c\,n} = nL_{c1}$. As the number of the flat segments increases, the perturbation amplitude of critical fluctuations does as well

$$\eta_{c\,n} = \frac{2n}{1 - \pi\gamma\, n} \quad \text{or} \quad \zeta_{c\,n} = \frac{2\beta}{\Delta\rho\, g}\, \frac{n}{L - L_{c\,n}}\,.$$

The potential barrier height grows as the number n of possible flat segments increases

$$\frac{\Delta E_n}{D} = \frac{2n^2}{1 - \pi\gamma\, n} = \frac{2\beta^2}{\Delta\rho\, g}\, \frac{n^2}{L - L_{c\,n}}\,.$$

Provided the experimental conditions correspond to the conservation of the total mass including the both liquid and solid phases, the solutions should satisfy an additional requirement

$$\int_{-L/2}^{L/2} \zeta(x)\, dx = 0.$$

In this case the nontrivial solutions for critical fluctuations can be realized for the even numbers n and, correspondingly, first critical length becomes equal to $L_{c\,2}$.

For the temperatures well below the roughening transition, the facet step energy coefficient β is measured [1], and the numerical estimate of the coefficient in Eq. (8) gives the magnitude of the potential barrier about 10^{-5} erg or 10^{11} K for the basal facet of size $\sim$1 cm. The overcoming of such barrier is practically impossible during the time of experiment. Thus, the appearance of the singular angle dependence in the function $\alpha(\theta)$ results in a drastic change for stability conditions of the crystal surface. With very small cooling below the roughening transition temperature the potential barrier becomes sufficiently large and the probability of its overcoming due to thermal or quantum fluctuations is vanishingly small. This conclusion is confirmed by the experimental evidence for stability of the crystal shape below the roughening transition.

The one-dimensional problem and boundary conditions (7) are chosen as simplest ones in order to illustrate the method of solution and to obtain an analytical estimate of the potential barrier height for developing gravitaional Rayleigh-like instability. The full problem should be solved employing the real crystal shape with the surfaces connecting the facets. We have analyzed an onset of instability at the circular facet on the analogy with Sec. IIC. The mathematical treatment becomes more complicated but the final result for the barrier height differs from Eq. (8) with a numerical coefficient of about unity.

B. Instability of the tilted crystal facet

Here we analyze the stability of a crystal facet tilted with angle $(\pi/2-\varphi)$ against its small perturbations. The variation of energy ΔE per width of the crystal facet reads

$$\frac{\Delta E}{D} = \int_{-L/2}^{L/2} dx \biggl(\frac{\alpha_0}{2}\,\zeta'^{\,2}(x) + \beta \mid \zeta'(x) \mid - \Delta\rho\, g\bigl(x\zeta(x)\cos\varphi + \frac{\zeta^2(x)}{2}\,\sin\varphi\bigr)\biggr), \quad (9)$$

where $\zeta(x)$ is a perturbation amplitude taken from the flat surface. The angle $\varphi = 0$ means the vertical position of the crystal and $\varphi = \pi/2$ corresponds to the horizontal position.

Let axis Oz run along the normal to the crystal facet. The axis Oy is perpendicular to the axis Oz and the acceleration of gravity as well. The third axis Ox, lying in the plane of the facet, is perpendicular to the axes Oy and Oz. The axis Ox runs at the angle φ to the direction of the acceleration of gravity.

Let perturbation amplitude of the crystal facet $\zeta(x)$ from its initial position $\zeta(x) = 0$ take place in the direction normal to the facet surface and be independent of the coordinate y directed horizontally along the crystal facet. In addition, we assume that the small perturbation amplitude $\zeta(x)$ is finite within the region $-L/2 < x < L/2$ and the following boundary conditions are fulfilled

$$\zeta(\pm L/2) = 0\,. \quad (10)$$

Here L is implied as a size of the crystal shape fluctuation. The surface fluctuations satisfy the conservation of the total mass of the liquid and solid phases

$$\int_{-L/2}^{L/2} \zeta(x)\,dx = 0\,. \quad (11)$$

For $\varphi = \pi/2$, expression (9) goes over to the expression for a horizontal crystal facet with the small vertical perturbations. For $\varphi = 0$, we have the expression for the energy of a vertical crystal facet with the small perturbations in the direction normal to the facet.

To find the minimum magnitude of the potential barrier which prevents from the development of instability, we must consider extremum of functional (9). The extremum of functional (9) satisfies the equation

$$\bigl(\alpha_0\zeta' + \beta\,\mathrm{sgn}\,\zeta'\bigr)' + \Delta\rho\, g\bigl(x\cos\varphi + \zeta\sin\varphi\bigr) = 0\,. \quad (12)$$

Provided the derivative $\zeta'(x)$ does not vanish for all x within $-L/2 < x < L/2$, i.e.,

$$\zeta'(x) \neq 0, \quad (13)$$

equation (12) takes the simple form

$$\alpha_0\zeta''(x) + \Delta\rho\, g\bigl(x\cos\varphi + \zeta(x)\sin\varphi\bigr) = 0\,. \quad (14)$$

If the condition (13) is satisfied, the general solution of Eq. (14) reads

$$\zeta(x) = -x\cot\varphi + A\sin(x/\lambda_\varphi) + B\cos(x/\lambda_\varphi). \quad (15)$$

Unknown coefficients A and B are determined by conditions (10) and (11). Finally, we arrive at

$$\zeta(x) = \left(\frac{\sin(x/\lambda_\varphi)}{\sin(L/2\lambda_\varphi)} - \frac{2x}{L}\right)\frac{L}{2}\cot\varphi\,. \quad (16)$$

Here λ_φ plays role of an effective capillary length and determines the typical scale of length at which $\zeta(x)$ varies

$$\lambda_\varphi = \sqrt{\frac{\alpha_0}{\Delta\rho\, g\sin\varphi}} = \frac{\lambda}{\sqrt{\sin\varphi}}\,.$$

Note that, as $\varphi \to 0$ for the vertical position of a crystal facet, the typical length λ_φ diverges.

Substituting (16) into (9), we have

$$\frac{\Delta E}{D} = \frac{\alpha_0}{2}\,\frac{\lambda_\varphi^3}{\lambda^2}\,\frac{\cos^2\varphi}{\sin\varphi}\int_{-\tilde{L}/2}^{\tilde{L}/2} dx \biggl(a^2\cos 2x - 2a\cos x + 1 + x^2 + 2(\beta/\alpha_0) \mid a\cos x - 1 \mid \tan\varphi\biggr) \quad (17)$$

Here we have introduced the dimensionless quantities

$$\tilde{L} = \frac{L}{\lambda_\varphi} \quad \text{and} \quad a = \frac{\tilde{L}/2}{\sin(\tilde{L}/2)}\,.$$

The magnitude of energy (17) can be written as

$$\frac{\Delta E}{D} = \frac{\alpha_0 L}{4}\,\frac{\lambda_\varphi^2}{\lambda^2}\,\frac{\cos^2\varphi}{\sin\varphi}\left(\frac{\tilde L^2}{6} - 2 + \tilde L\cot\frac{\tilde L}{2}\right) + \beta\,\frac{\lambda_\varphi^3}{\lambda^2}\,\cos\varphi\int_{-\tilde L/2}^{\tilde L/2} dx\mid a\cos x - 1\mid . \quad (18)$$

For $\tilde L = L/\lambda_\varphi \ll 1$, equation (18) gives

$$\frac{\Delta E}{D} = -\frac{\alpha_0 L}{80}\,\cot^2\varphi\left(\frac{L}{2\lambda_\varphi}\right)^4 + \frac{\beta L}{12}\cot\varphi\left(\frac{L}{2\lambda_\varphi}\right)^2 .$$

As a result, for sufficiently small-sized fluctuations with $L \ll L_{cr}$, the energy of fluctuations is positive $\Delta E > 0$ and such fluctuations are of low probability. The tilted facet is practically stable for such perturbations. The critical length is equal to

$$L_{cr} = 4\,\lambda_\varphi\sqrt{\frac{5\beta}{3\alpha_0}\,\tan\varphi} = \frac{4\sqrt{5\beta/(3\Delta\rho\, g)}}{\sqrt{\cos\varphi}}\,.$$

This means that the crystal facet is practically stable if its size does not exceed the critical length. In fact, the magnitude of the energy barrier $\Delta E \sim \beta^2/\Delta\rho\, g$ proves to be about 10^{-5} erg or 10^{11} K. As the size of a crystal becomes larger than the critical length $L > L_{cr}$, the tilted crystal facet becomes unstable against distortion of its shape.

The analysis of the crystal facet stability for the larger lengths $L \sim \lambda_\varphi$ is simple. Let us represent Eq. (18) in the form of the following inequality

$$\frac{\Delta E}{D} \leqslant \frac{\alpha_0 L}{4}\,\frac{\lambda_\varphi^2}{\lambda^2}\,\frac{\cos^2\varphi}{\sin\varphi}\left(\frac{\tilde L^2}{6} - 2 + \tilde L\cot\frac{\tilde L}{2}\right) + \beta\,\frac{\lambda_\varphi^3}{\lambda^2}\,\cos\varphi\left(\int_{-\tilde L/2}^{\tilde L/2} dx\,(\mid a\cos x\mid +1)\right).$$

The right-hand side of the inequality is obviously negative for $\tilde L \gtrsim \pi$, i.e. $\Delta E < 0$. This means that a crystal facet distortion with such lengths is energetically favorable. The tilted crystal facet becomes absolutely unstable if the facet size $L \gtrsim \lambda_\varphi$.

In conclusion, such high potential barriers can explain a gravitational stability of a crystal facet in the immediate vicinity of the roughening transition temperature at which the facet step energy vanishes (Fig. 4). In Fig. 4 the image of a ^{4}He crystal at 0.901 K is given. Note that the lateral faceting disappears at 0.910 K, demonstrating the roughening transition for the a-facets. The crystal has a clear lateral facet which remained stable in the course of experiment during, at least, 10 min.

IV. CONCLUSION

The gravitational instability at the atomically rough ^{4}He surface, which develops under the lack of any potential barrier, is similar to the classical Rayleigh instability

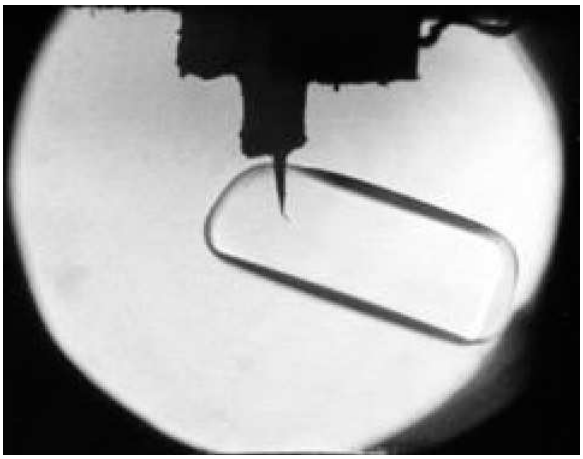

FIG. 4: The lateral facet of a ^{4}He crystal is stable. The temperature is below the second roughening transition by about 20 mK.

when the heavier liquid lies above the lighter liquid. The distinction is that the time necessary for the development of instability is determined by the kinetic growth coefficient of a crystal surface.

As for the smooth faceted crystal surface, having a singularity in the surface stiffness, the development of the surface instability becomes possible due to thermal or quantum fluctuations if the size of the facet surface exceeds the critical one. However, the large height of a potential barrier makes its overcoming impossible for a experimentally reasonable time. This explains the stability of the lower facet for a free-growing ^{4}He crystal observed in the experiment during a few hours.

[1] S. Balibar, H. Alles, and A. Ya. Parshin, Rev. Mod. Phys. **77**, 317 (2005).

[2] C. D. Demaria, J. W. Lewellen, and A. J. Dahm, J. Low Temp. Phys. **89**, 385 (1992).

[3] V. L. Tsymbalenko, Fiz. Nizk. Temp. **21**, 162 (1995) [Low Temp. Phys. **21**, 120 (1995)].

[4] A. F. Andreev and A. Ya. Parshin, Zh. Eksp. Teor. Fiz. **75**, 1511 (1978) [Sov. Phys. JETP **48**, 763 (1978)].

[5] A. O. Keshishev, A. Ya. Parshin, and A. V. Babkin, Zh. Eksp. Teor. Fiz. **80**, 716 (1981) [Sov. Phys. JETP **53**, 362 (1981)]. **114**, 1313 (1998) [JETP **87**, 714 (1998)].

[6] L. D. Landau, *The Equilibrium Form of Crystals*, in Collected Papers (Pergamon, Oxford, 1965).